

Available online at [www.sciencedirect.com](http://www.sciencedirect.com)

ScienceDirect

[www.elsevier.com/locate/jmbbm](http://www.elsevier.com/locate/jmbbm)

## Research Paper

# Giant panda's tooth enamel: Structure, mechanical behavior and toughening mechanisms under indentation

Z.Y. Weng<sup>a</sup>, Z.Q. Liu<sup>a,b,\*</sup>, R.O. Ritchie<sup>b</sup>, D. Jiao<sup>a</sup>, D.S. Li<sup>c</sup>, H.L. Wu<sup>c</sup>, L.H. Deng<sup>c</sup>, Z.F. Zhang<sup>a,\*</sup>

<sup>a</sup>Shenyang National Laboratory for Materials Science, Institute of Metal Research, Chinese Academy of Sciences, Shenyang 110016, China

<sup>b</sup>Department of Materials Science and Engineering, University of California, Berkeley, CA 94720, USA

<sup>c</sup>China Conservation & Research Centre for the Giant Panda, Wolong 623003, China

## ARTICLE INFO

## Article history:

Received 6 June 2016

Received in revised form

12 July 2016

Accepted 24 July 2016

Available online 29 July 2016

## Keywords:

Giant panda

Tooth enamel

Hierarchical structure

Indentation

Anisotropy

Toughening mechanisms

## ABSTRACT

The giant panda's teeth possess remarkable load-bearing capacity and damage resistance for masticating bamboos. In this study, the hierarchical structure and mechanical behavior of the giant panda's tooth enamel were investigated under indentation. The effects of loading orientation and location on mechanical properties of the enamel were clarified and the evolution of damage in the enamel under increasing load evaluated. The nature of the damage, both at and beneath the indentation surfaces, and the underlying toughening mechanisms were explored. Indentation cracks invariably were seen to propagate along the internal interfaces, specifically the sheaths between enamel rods, and multiple extrinsic toughening mechanisms, *e.g.*, crack deflection/twisting and uncracked-ligament bridging, were active to shield the tips of cracks from the applied stress. The giant panda's tooth enamel is analogous to human enamel in its mechanical properties, yet it has superior hardness and Young's modulus but inferior toughness as compared to the bamboo that pandas primarily feed on, highlighting the critical roles of the integration of underlying tissues in the entire tooth and the highly hydrated state of bamboo foods. Our objective is that this study can aid the understanding of the structure-mechanical property relations in the tooth enamel of mammals and further provide some insight on the food habits of the giant pandas.

© 2016 Elsevier Ltd. All rights reserved.

\*Corresponding authors at: Shenyang National Laboratory for Materials Science, Institute of Metal Research, Chinese Academy of Sciences, Shenyang 110016, China. Fax: +0086 24 23891320.

E-mail addresses: [zqliu@berkeley.edu](mailto:zqliu@berkeley.edu) (Z.Q. Liu), [zhfzhang@imr.ac.cn](mailto:zhfzhang@imr.ac.cn) (Z.F. Zhang).

## 1. Introduction

Enamel, the outermost layer of a tooth crown, plays a critical role in accomplishing the oral functions and protecting the underlying dentin and pulp chamber from mechanical damage. As the most highly mineralized tissue in mammals, enamel is mainly composed of hydroxyapatite (HAP) mineral crystals (~96 wt%) and a small fraction of protein and water (~4 wt%) (Nanci, 2008). Similar to other biological materials, enamel possesses a complex hierarchical structure spanning several length-scales. As with most enamels in mammals, the nanosized fiber-like HAP crystals are glued together by protein (mainly hydrophobic enamelins) to form the fundamental structural units of enamel at the micrometer-level which are termed as “rods” or “prisms” (Cui and Ge, 2007). These rods are separated and surrounded by protein-rich sheaths, primarily comprising acidic proteins, enamelins, and tuftelins (He and Swain, 2008), and are believed to extend from the dental-enamel junction (DEJ) to the occlusal surface in enamel. Such structural complexity and hierarchy render the enamel with unique mechanical properties, especially fracture resistance, that are superior compared to its principal component, HAP mineral, to fulfill its mechanical demand for mastication of millions of times during the lifetime of the organisms (Bajaj et al., 2008; Cui and Ge, 2007; He and Swain, 2008; Macho et al., 2003).

Tooth enamel has attracted intensive research interest owing to its significance for clinical tooth preparation and protection as well as dental restoration. The structure of enamel has been well described for the teeth of human and some kinds of animals; the detailed characteristics, though, i.e., the arrangement and dimension of its structural units, can vary among different species of organisms (Koenigswald and Clemens, 1992; Maas and Dumont, 1999). Because of the small size and irregular shape of tooth enamel, indentation has been most frequently adopted to determine the mechanical properties that are physiologically vital for its function. A suite of mechanical properties of enamel, including hardness, elastic modulus and fracture toughness, have been determined by indentation with a series of toughening mechanisms, e.g., microcracking and uncracked-ligament bridging, identified to shield cracks from the applied stress (Ang et al., 2011; Bajaj et al., 2010; Craig and Peyton, 1958; Gutiérrez-Salazar and Reyes-Gasga, 2003; Habelitz et al., 2001; Hassan et al., 1981; He et al., 2006; Imbeni et al., 2005; Mann and Dickinson, 2006; Park et al., 2008a, 2008b; Shang and Ritchie, 1989; Staines et al., 1981; Xu et al., 1998). Nevertheless, whereas the damage on the indentation surface has been principally analyzed in previous studies (Ang et al., 2011; Bajaj et al., 2010; Chai et al., 2011; Hassan et al., 1981; Kruzic et al., 2009; Xu et al., 1998), the damage behavior and toughening mechanisms in enamel beneath the indenter still remain unclear. Indeed, many tiny flaws or cracks can form in the enamel caused by high-cycle occlusion, temperature variation, corrosion or decay. Despite this, the tooth enamel retains its mechanical function without catastrophic failure even as such damage develops, highlighting the necessity to explore the sub-surface mechanical behavior and toughening mechanisms in this material. Moreover, as the enamel

displays anisotropic mechanical properties owing to the unique arrangement of structural units (Braly et al., 2007; Habelitz et al., 2001), the orientation dependence of the indentation behavior beneath the occlusal surface still remains to be clarified.

Giant pandas (*Ailuropoda melanoleuca*), which inhabit the mountain ranges in central China, are famous as a conservation reliant endangered species. Unlike other bears, they feed almost exclusively on bamboo (Fig. 1a). Bamboo, especially its stems, possesses a remarkable combination of high stiffness, strength and fracture toughness; specifically, its specific tensile strength is some six times higher than that of mild steel (Amada et al., 1997; Amada and Untao, 2001). The giant panda's tooth enamel is more likely to surpass bamboo in terms of its mechanical properties as it remains intact under direct impact during mastication. Accordingly, the prime objective of this study is to clarify the structure and mechanical behavior of the enamel in the teeth of giant pandas under indentation, by monitoring the evolution of damage under increasing load and defining how its mechanical properties vary by location and orientation, in order to reveal the underlying toughening mechanisms and their structural origins. This study is expected to also provide insight on the food habits of the giant pandas and help discern the structure-property relationships in tooth enamel.

## 2. Materials and methods

A set of dried jaws were extracted from the skeleton of a giant panda that had died naturally at the Conservation & Research Centre for the Giant Panda, Wolong, China. The third and fourth premolars on both chewing sides, which were free of dental caries and maintained a better state compared to other teeth, were cut from the lower jaw using a diamond band saw. These premolars have been shown to play an essential role in accomplishing the foraging and mastication functions, such as cutting and tearing bamboos, and thus are critical for the giant pandas (Huang, 1993). Using the nomenclature that orientations which are perpendicular and parallel to the occlusal surface are denoted as longitudinal and transverse, respectively, a third premolar was sectioned along the longitudinal plane normal to the lingual-buccal direction using a low-speed diamond wire saw. The resulting sections and the occlusal surface of the other third premolar were carefully ground using abrasive papers and polished to ~0.5 μm finish, and then etched with 10 wt% H<sub>3</sub>PO<sub>4</sub> solution for 1 min. The samples were examined using an Olympus LEXT OLS 4000 3D-measuring microscope, and then sputter-coated with a thin film of gold and observed by field emission scanning electron microscopy (SEM) in the secondary electron mode at an accelerating voltage of 10 kV using an LEO Supra 55 instrument. Electron probe microanalysis (EPMA) was performed on the longitudinal section at different positions along the thickness of enamel using an EPMA-1610 electron probe microanalyzer operating at an accelerating voltage of 10 kV with a beam of 1 μm diameter.

For transmission electron microscopy (TEM) observations, thin longitudinal sections were cut from the enamel using the wire saw and carefully ground to a thickness of ~40 μm.

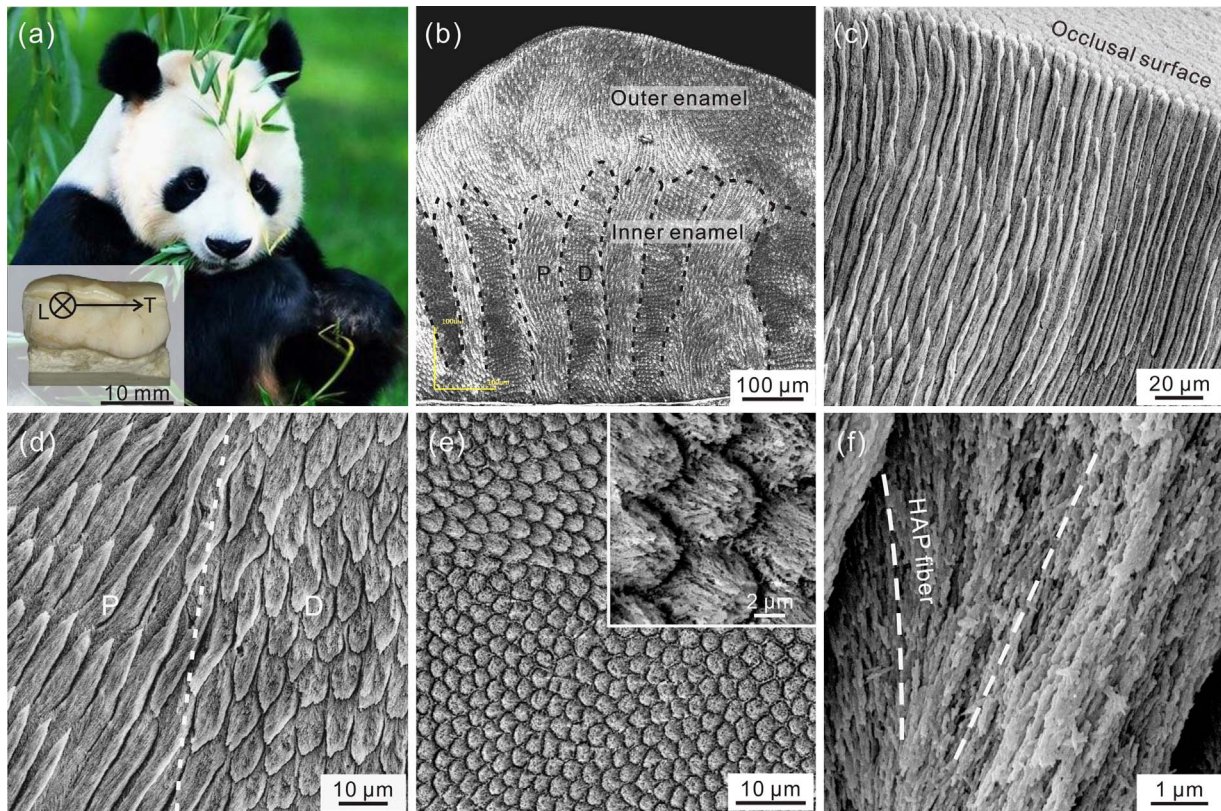


**Fig. 1 – (a) Macroscopic images of a giant panda chewing bamboo and a third premolar used in this study (inset). (b) Optical micrograph of the longitudinal section of giant panda's tooth enamel. The boundary between outer and inner enamels is denoted by the dashed curve. The boundaries between the P- and D-zones in the inner enamel are denoted by the dotted curves. (c–e) SEM micrographs of the outer (c) and inner (d) enamels as well as the etched occlusal surface (e). (f) SEM micrograph of the HAP fibers within an enamel rod.**

The samples were polished using a precision ion polishing system (Model 691, Gatan) at 5 kV with successively decreasing inclination angle from 18° to 15° until a small hole appeared in the center, and then were further thinned at 5 kV with inclination angle of 5° for 30 min. The specimens were observed using a field emission G2 F20 Tecnai TEM instrument at an accelerating voltage of 200 kV.

For mechanical characterization, a fourth premolar was sectioned longitudinally along the lingual-buccal direction. The longitudinal section of one half and the occlusal surface of the other half of enamel were manually ground and polished in the same manner described above. All the samples were dried in air at room temperature for at least 12 h prior to the mechanical testing. Indentation testing was performed on the occlusal surface under a series of loads of 50, 100, 200, and 500 gf, and on the longitudinal section at different positions from occlusal surface to DEJ using 200 gf load with a dwell time of 30 s using a Vickers microhardness tester (VH-5ACL). At least five measurements were conducted for each case to obtain the average and standard deviation so that the data reproducibility was ensured.

The other fourth premolar was divided into several blocks comprising the cuspal enamel using the wire saw. After grinding and polishing the occlusal surfaces, some blocks were sectioned along the longitudinal direction. The opposite

faces of the resulting two halves were ground and polished, and then clamped together using a clip. The clamped occlusal surface was indented under varying loads of 50–500 gf with a dwell time of 30 s. The halves were subsequently separated by removing the clip to expose the morphologies beneath the indenter. Although the stress state in the clamped sample may be affected by the presence of an interface, such technique has been widely applied as it readily unveils the subsurface deformation behavior of samples under indentation (Cai et al., 1994; Jung et al., 1999; Liu et al., 2016; Ramamurty et al., 2005). To explore the effect of loading orientation, indentation testing was also performed on the clamped longitudinal section, i.e., loaded along the transverse direction. In this case, only a 200 gf load was utilized due to the limited enamel thickness. After indentation, all samples were sputter-coated with gold film and analyzed by SEM. Nanoindentation testing was conducted on the polished occlusal surface and longitudinal section under displacement-control mode using a three-sided Berkovich indenter on Agilent Nano Indenter G200 machine. The displacement rate and the maximum depth were set as 10 nm/s and 250 nm, respectively, with 14 repeated tests for each case. Each test lasted for approximately 230 s with the hold time at the peak load set as 10 s. The Poisson's ratio of tooth enamel was taken as 0.3 (Haines, 1968).

### 3. Results

#### 3.1. Structure of giant panda's tooth enamel

Fig. 1a shows the macroscopic appearance of a giant panda masticating bamboo. The inset shows an extracted third premolar, the dimension of which is  $\sim 19$  mm in length and  $\sim 11$  mm in width; the height of the exposed dental crown is  $\sim 6$  mm. The giant panda's tooth enamel is composed of a mass of micrometer-scale rods or prisms (Fig. 1b). The arrangement of rods differs markedly at different thickness in the enamel; consequently, the tissue can be categorized into outer and inner enamel regions. In the outer enamel, the rods are well aligned and extend towards the occlusal surface (Fig. 1c). In contrast, the inner enamel comprises alternating decussation bands where the rods are obliquely oriented (Fig. 1d). Two characteristic zones, referred to as para-zones (P) and dia-zones (D) (Mortell and Peyton, 1956; Wang et al., 2012), can be distinguished where the rods appear to have been cut, respectively, more longitudinally and transversely. The etched occlusal surface displays a fish scale-like pattern with the cross section of individual rods with a so-called keyhole-type shape (Fig. 1e). The equivalent diameter of the enamel rods was measured to be  $5.4 \pm 0.3 \mu\text{m}$ . At the lower length-scale, the enamel rods were constituted by nanosized

fibers of HAP crystallites with an orientation which continuously changes within the rods.

The constituent fibers within enamel rods were measured to have a diameter of  $35 \pm 10$  nm with a length much larger than  $1 \mu\text{m}$  (Fig. 2). These fibers are well aligned in the center of enamel rods and fan out towards the rod boundaries at the periphery. The deviation angle lies from  $\sim 8^\circ$  on one side to  $\sim 25^\circ$  on the other within the rod (Fig. 2a and b). The inter-rod regions, or sheaths, have a thickness of  $\sim 64$  nm (Fig. 2b). The boundaries of these sheaths are microscopically uneven and some of the fibers may extend from neighboring rods and intersect there. The hexagonal apatite phase structure of the constituent fibers was confirmed by high-resolution TEM and corresponding fast Fourier transformation patterns of an isolated single crystal (Fig. 2c). The long axis of fibers corresponds well to the [0001] crystallographic orientation of the HAP crystals.

The structure of giant panda's tooth enamel can be schematically illustrated in Fig. 3. The nano-scale HAP crystallite fibers, as the first-order structural element, are bundled together to form the higher-level hierarchy, the enamel rods, of which the unique arrangements, specifically their varying orientations, lead to the outer and inner enamels and the decussation bands within the latter on the larger length-scale. The structural complexity and hierarchy have been clarified for the tooth enamels of human and a variety of animals (Cui and

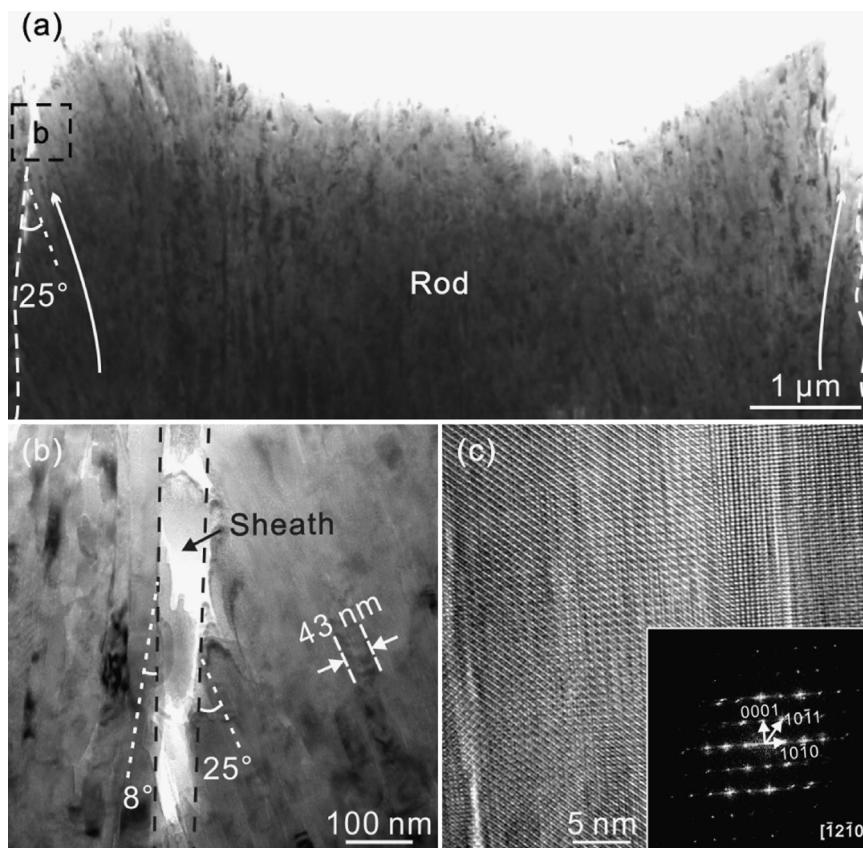


Fig. 2 – (a, b) TEM micrographs of one enamel rod (a) and the sheath between adjacent rods (b). The orientations of HAP fibers at the periphery of rod are denoted by the dotted lines in (b). (c) High-resolution TEM micrograph of one HAP fiber and corresponding fast Fourier transformation pattern.

Ge, 2007; Koenigswald and Clemens, 1992; Maas and Dumont, 1999). The tooth enamel structure of giant panda is analogous to those of human and some other animals, e.g., Rodentia and Carnivora, especially to that of the common bear *Ursus speleaus* (Koenigswald

and Clemens, 1992). The primary difference lies in the characteristic dimensions of the structural hierarchies. For instance, the diameter of the enamel rod of *Alagomys inopinatus* (~3 μm) is markedly smaller than that of giant panda (Martin, 1993). Besides, despite a similar size of enamel rods, the diameter of

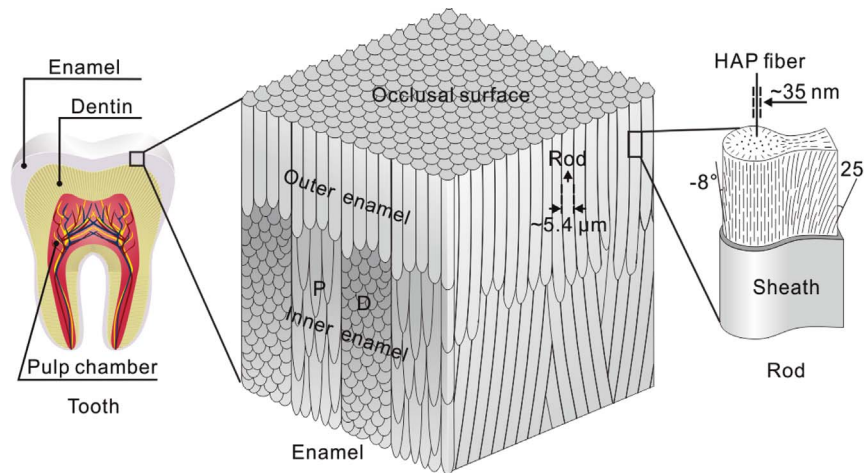


Fig. 3 – Schematic illustrations of the hierarchical structure of giant panda's tooth enamel.

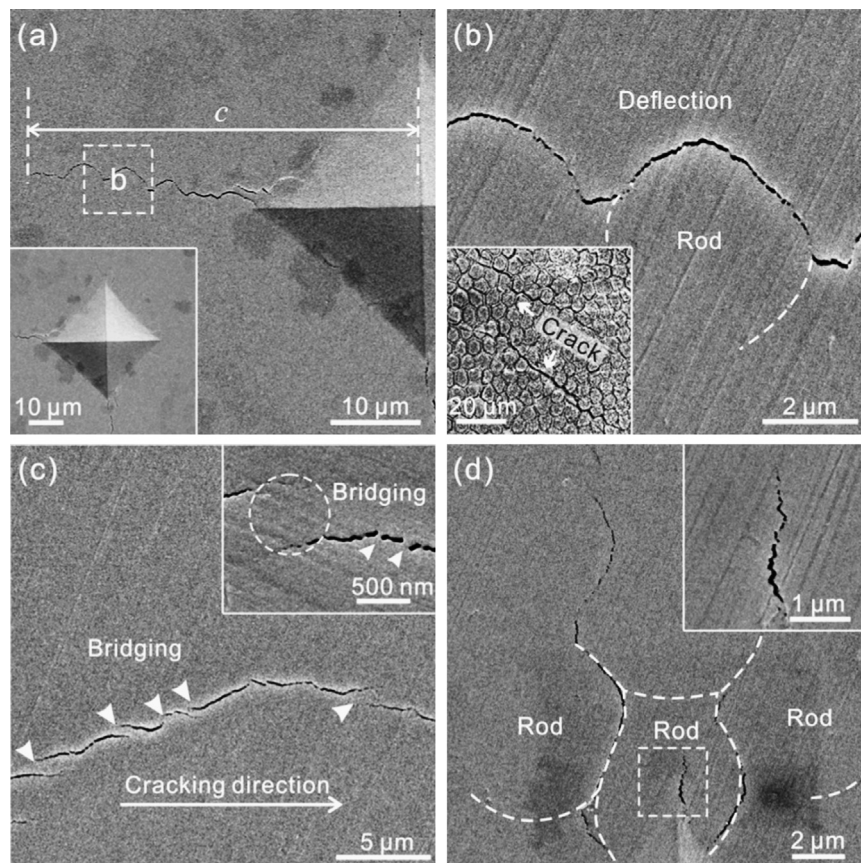


Fig. 4 – SEM micrographs of the polished occlusal surface of giant panda's tooth enamel after indentation under 200 gf load along the longitudinal direction. The crack length  $c$  used to calculate indentation toughness is denoted in (a). The square region in (a) is magnified in (b). The inset in (b) shows the optical image of indentation cracks on etched occlusal surface where the rod boundaries can be easily distinguished. The square region in (d) is magnified as inset. The boundaries between enamel rods are indicated by dashed curves.

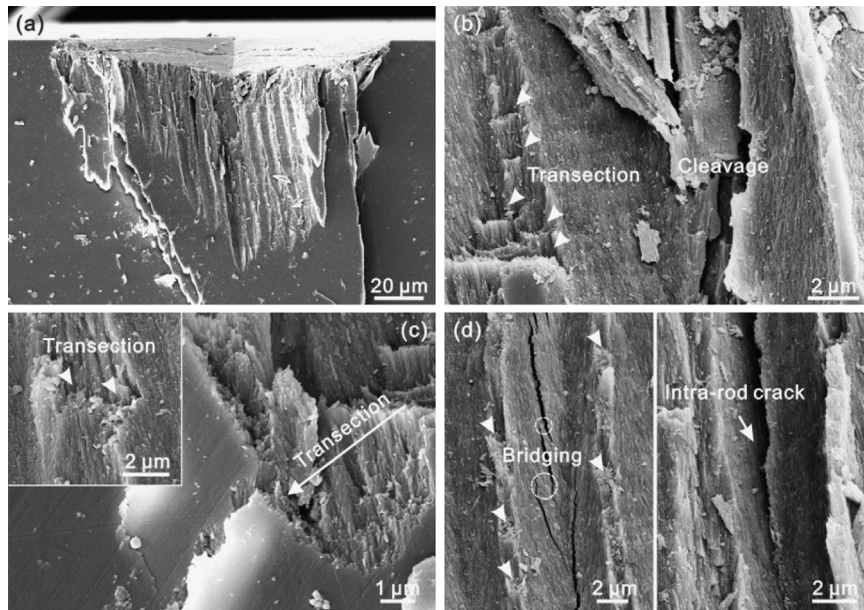


Fig. 5 – SEM micrographs of giant panda's tooth enamel beneath the indenter after indentation under 200 gf load along the longitudinal direction. (b–d) show magnified views of representative morphologies manifesting the propagation of inter- and intra-rod cracks.

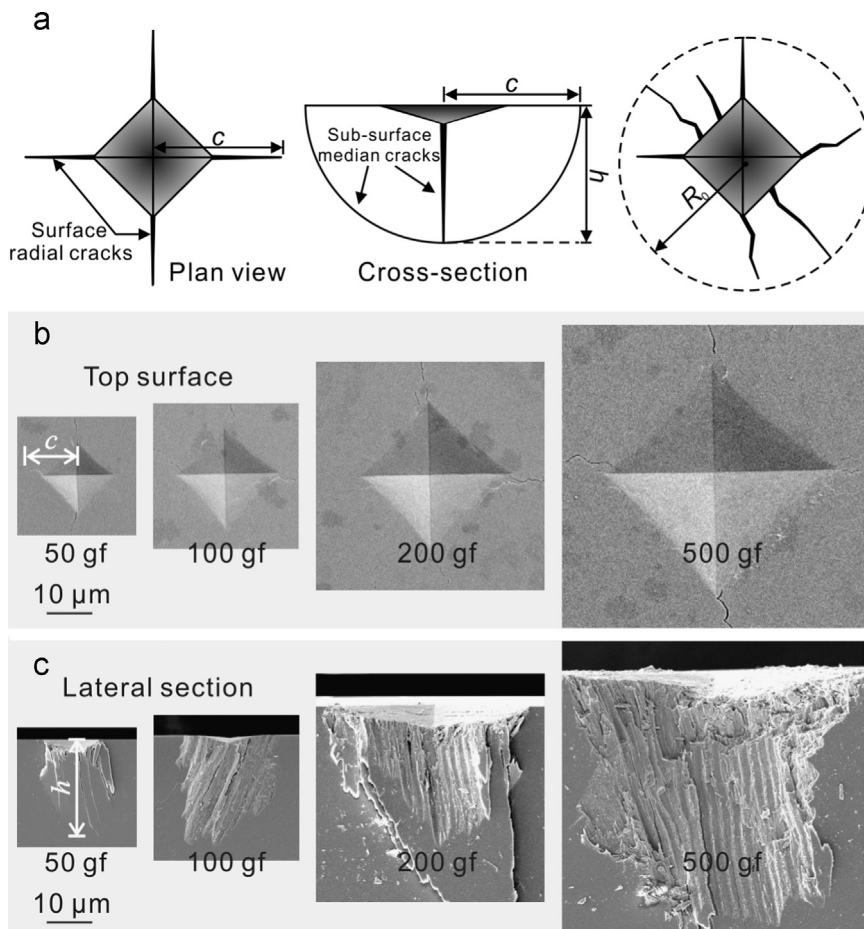


Fig. 6 – (a) Schematic illustrations of the indentation cracks and their characteristic dimensions. (b, c) SEM micrographs of the top surfaces (b) and lateral sections (c) of giant panda's tooth enamel after indentation with increasing load along the longitudinal direction.

the involved HAP fibers is slightly larger in human tooth enamel (~43 nm) than in the giant panda (Daculsi and Kerebel, 1978).

### 3.2. Indentation behavior along longitudinal direction

The mechanical behavior of giant panda's tooth enamel was first examined by indenting the occlusal surface along the longitudinal direction, which is representative of the loading condition causing general radial-median cracks during mastication (Barani et al., 2011). The hardness was measured to be  $3.37 \pm 0.06$  GPa, that is close to that of dried human enamel (~3.20–4.16 GPa) (Craig and Peyton, 1958; Gutiérrez-Salazar and Reyes-Gasga, 2003). As shown in Fig. 4, radial-median cracks emanated from the indenter corners due to the stress concentration and the normal stress-state here. The fracture toughness  $K_C$  can be approximately evaluated from the mean indentation crack length  $c$ , defined as the distance from the crack tip to the crater center, following the expression:

$$K_C = \chi(E/H)^{1/2}P/c^{3/2}, \quad (1)$$

where  $P$  is the indentation load and the parameter  $\chi$ , termed as the geometric constant of indenter, equals to 0.016 (Anstis et al., 1981).  $E$  and  $H$  represent the Young's modulus and hardness of the enamel, respectively. Of note here is that the indentation cracks in biological materials are generally not straight or symmetric as in brittle materials with linear-elastic fracture mechanics behavior. The average crack length has been adopted despite the curvatures and bridging ligaments occurring during the propagation of cracks; such method has been widely applied to evaluate the fracture toughness of various biological materials, including nacreous shell (Jiao et al., 2015; Li and Ortiz, 2014) and tooth enamel (Bajaj et al., 2010; Park et al., 2008a, 2008b; Xu et al., 1998). The Young's moduli of the outer enamel along the longitudinal and transverse directions were measured to be  $106 \pm 4$  GPa and  $96 \pm 1$  GPa, respectively, by nanoindentation testing. This gives values of  $K_C$  of  $0.52 \pm 0.11$  MPa  $m^{1/2}$  along the longitudinal direction, which is similar to the reported toughness of the outer enamel in human teeth that ranges from 0.4 to 1.0 MPa  $m^{1/2}$  (Bajaj et al., 2010; Hassan et al., 1981; Park et al., 2008a, 2008b; White et al., 2001); both are superior to the corresponding toughness of the HAP mineral, which has been measured to be  $\sim 0.3$  MPa  $m^{1/2}$  (Bajaj et al., 2008).

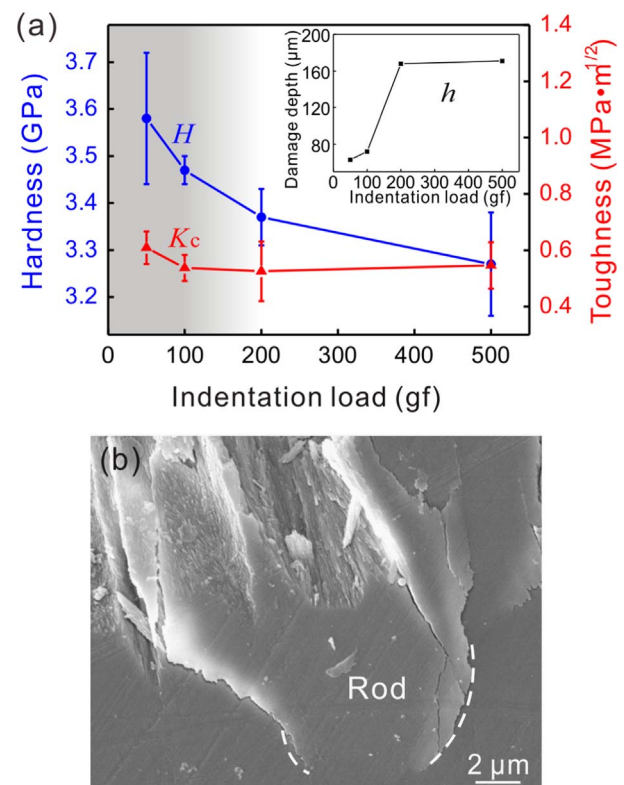
The indentation cracks preferentially originate and propagate along the interfaces between the rods (sheaths), resulting in marked crack deflection along fairly wavy trajectories, with multiple uncracked ligaments forming along the crack path. Such ligaments act to bridge the crack and carry load, which would otherwise be used to promote crack propagation, thus shielding the crack tip from applied stress. Similar to the bovine enamel (Ang et al., 2011), crack bridging operates at micrometer to nanometer length-scales, specifically corresponding to rods and bundles of different numbers of HAP fibers. Intra-rod cracks occasionally formed at the indenter corner due to the stress concentration, yet these cracks were more easily arrested within the rods owing to the efficient deflection and bridging at the nanoscale of HAP fibers.

Fig. 5 shows the damage morphologies of the giant panda's tooth enamel beneath the indenter. The enamel

displays distinct damage features which vary with the distance from the indenter. Multiple inter- and intra-rod cracks, corresponding primarily to the separation between rods and HAP fibers, respectively, were formed in the zone adjacent to crater. The inter-rod cracks tend to propagate inwards along the sheaths, resulting in marked crack deflection and twisting. By comparison, the intra-rod cracks were easily channeled along the fiber boundaries and bridged by the intact fibers or fiber bundles, such that tilting of fibers within rods led to continuous crack deflection along them. As such, these cracks were more prone to be arrested within the rods. Alternatively, they sometimes converged into inter-rod cracks by transecting the HAP fibers, leading to a series of steps. With such arrest and convergence of intra-rod cracks, the damage becomes dominated by the interfacial cracking between rods in deeper region of the enamel.

### 3.3. Damage evolution with increasing load

The damage evolution of giant panda's tooth enamel was accessed by comparing the indentation behavior at increasing loads. The extent of damage was described using the indentation crack length  $c$  and depth  $h$  on the top and lateral surfaces, respectively, as shown in Fig. 6. It is noted that  $h$  was determined as the depth of cracked region, rather than



**Fig. 7 – (a) Variations in measured hardness and indentation toughness as a function of applied load by indentation with increasing load along the longitudinal direction. The dependence of damage depth  $h$  on the indentation load is shown in the inset. (b) Magnified morphology in the sample indented under 500 gf load showing the out-of-plane twisting of inter-rod cracks in the inner enamel.**

**Table 1 – Hardness and indentation toughness of giant panda's tooth enamel measured by indentation under 200 gf load at different positions along longitudinal and transverse directions. The t-test results under a significance level of 0.05 are presented for corresponding data sets.**

Orientation	Longitudinal	Transverse	Inner enamel	P-zone	D-zone
Position	Outer enamel	Outer enamel			
Hardness (GPa)	3.37 ± 0.06	3.45 ± 0.04	3.22 ± 0.09	3.16 ± 0.09	3.24 ± 0.05
Calculated t and Standard t	2.648 and 2.179 (Significant)		5.551 and 2.101 (Significant)		2.018 and 2.132 (Insignificant)
Toughness (MPa m <sup>1/2</sup> )	0.52 ± 0.11	0.64 ± 0.06	0.93 ± 0.08	0.92 ± 0.08	0.93 ± 0.08
Calculated t and Standard t	2.218 and 2.201 (Significant)		7.452 and 2.145 (Significant)		0.233 and 2.201 (Insignificant)

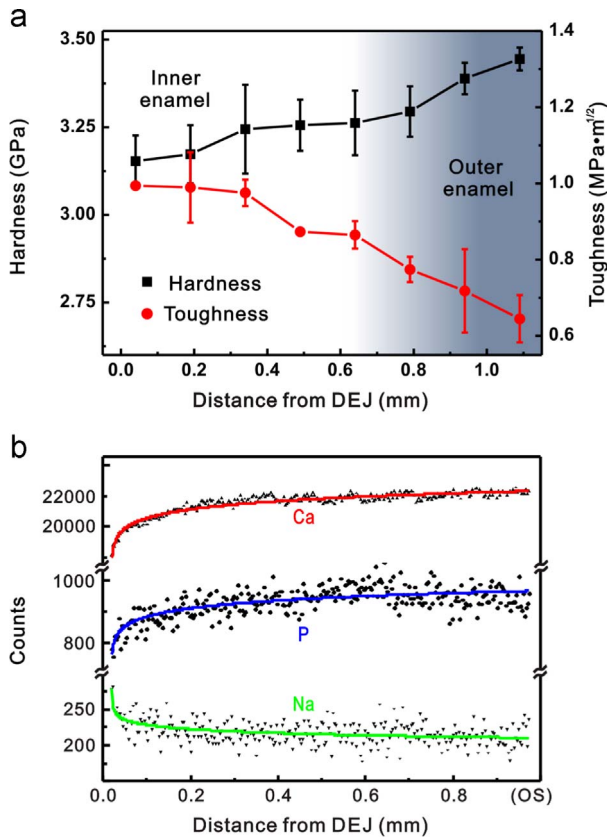


**Fig. 8 – (a) Variations in hardness and indentation toughness along the transverse direction as a function of the distance from the DEJ towards the occlusal surface. (b) Distributions of elements Ca, P and Na across the enamel thickness. OS is short for occlusal surface.**

the fragmented one, when not the entire damaged zone was fractured. The resulting hardness displays a decreasing trend with the increase in applied load, yet the indentation toughness remains relatively constant (Fig. 7a).

The trend of the progressive increase in indentation depth  $h$  with increasing load is reduced as the load exceeds 200 gf (inset of Fig. 7a), an observation that corresponds to where the indentation cracks encounter the inner enamel as they propagate inwards. As described above (Section 3.1), the inner enamel consists of alternating decussation bands within which the rods are continuously tilted with varying orientations. The complex interfaces between the rods, as opposed to the straight longitudinal ones in the outer enamel, lead to

marked twisting and deflection of inter-rod cracks along them, as represented by the out-of-plane propagation of cracks along sheaths (Fig. 7b). Such a crack-deflection mechanism enhances the extrinsic toughening effect by directing crack trajectories away from the path of maximum mechanical driving force, thereby contributing to a higher resistance against the inward development of indentation damage. This trend also conforms to previous reports that the inner enamel has a higher toughness than the outer enamel; furthermore, it is consistent with the rising crack-growth-resistance behavior displayed by the enamel region (Bajaj and Arola, 2009). Here the transition depth between the outer and inner enamels ( $\sim 170 \mu\text{m}$ ) is lower compared to the thickness of the outer enamel (Fig. 1b) as a result of specimen preparation, specifically from surface grinding and polishing.

#### 3.4. Indentation behavior along transverse direction

The indentation behavior of giant panda's tooth enamel along the transverse direction was analyzed and compared to that on the occlusal surface, as listed in Table 1. Statistical t-tests were performed to examine whether differences between the mechanical properties corresponding to different orientations and positions were statistically significant. There exists significant difference when the calculated  $t$  is larger than standard  $t$ , and vice versa. The statistics show that the outer enamel possesses significantly higher hardness and indentation toughness along the transverse direction as compared to the longitudinal one, signifying marked mechanical anisotropy. With respect of the location-dependent properties, the inner enamel is significantly tougher yet displays a lower hardness than the outer enamel. This is actually the characteristic design of a wear or impact-resistant material with a hard surface layer to resist surface damage and/or penetration coupled with a softer and tougher lower layer to accommodate any excess deformation; such a concept is common in Nature, for example in the structure of armored fish scales and mollusk shells (Amini and Miserez, 2013; Chen et al., 2008a, 2008b; Jiao et al., 2015).

The variations of mechanical properties as a function of the distance away from DEJ are shown in Fig. 8a.<sup>1</sup> It can be seen that the hardness increases monotonically towards the

<sup>1</sup>Note that the indentation crack length  $c$  was determined as the radius of damaged zone,  $R_0$ , by using the smallest circle enclosing the damage for samples where the cracks did not strictly emanate from the indenter corners, as shown in Fig. 6a, in a similar manner to that described by Li and Ortiz (2014).

occlusal surface, while the indentation toughness varies in the opposite fashion, consistent with trends reported for human tooth enamel (Cuy et al., 2002; Gutiérrez-Salazar and Reyes-Gasga, 2003; Imbeni et al., 2005). Such variations would appear to be associated with the heterogeneous chemical composition. Specifically, the Ca and P concentrations in HAP mineral decrease gradually from the occlusal surface towards DEJ (Fig. 8b), implying a gradient in mineralization across the enamel. Despite the distinct structural orientations, no differences in the mechanical properties between P- and D-zones within the inner enamel were found to be statistically significant.

Fig. 9 shows representative indentation morphologies of the outer enamel and the P- and D-zones within the inner enamel. In contrast to the isotropic corner cracks on occlusal surface, the damage preferentially develops along the longitudinal direction, i.e., the long axis of rods, in the outer enamel. Analogously, the propagation of cracks is hindered by a series of crack-tip shielding mechanisms, such as crack deflection and uncracked-ligament bridging, which particularly cause the intra-rod cracks to be arrested when act at the nanoscale. In comparison, the inner enamel displays distinctly different damage features in the P- compared to the D-zones. In the P-zone where the enamel rods are tilted towards out-of-plane, the rods fragmented and the resultant cracks were widely distributed rather than to be confined near the indenter corners. However, in the D-zone, inter-rod cracks were formed and deflected along the rod interfaces, akin to the cracking configurations in the longitudinal direction.

The damage morphologies beneath the indenter of outer enamel are shown in Fig. 10. The damage depth was about one fourth of that measured for the longitudinal direction under the same load. Despite the severe crushing in the zone adjacent to the indenter, cracks emanating from the indent tended to be channeled nearly transversely along the rod interfaces or along the boundaries between HAP fibers within rods, leading to marked crack deflection and crack bifurcation. By comparison, the inward development of indentation damage necessitates the cracks to traverse the enamel rods, which results in higher resistance to crack advance. As such, the cracks are more easily arrested, leading to the confinement of indentation damage within a lower depth, compared to indentation along longitudinal direction.

## 4. Discussion

### 4.1. Structural dependence of indentation behavior

The indentation behavior of giant panda's tooth enamel depends on both structural orientation and location. The lower hardness and indentation toughness along the longitudinal direction, as compared to the transverse direction, appear to be associated with the consistence between the orientation of sheaths and the loading direction. As such, deformation and damage are more prone to occur through plastic shearing or cracking along the sheaths, which because of their high organic content are weaker (Bechtle et al., 2010a,

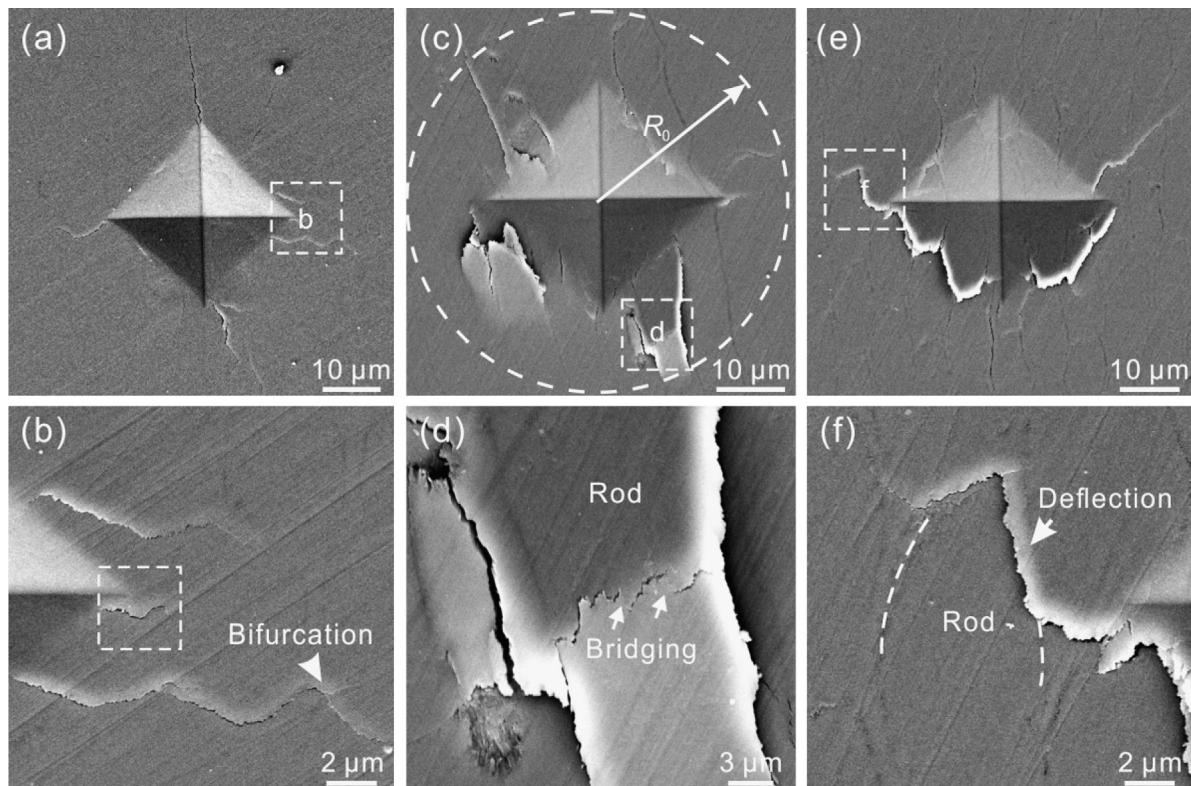
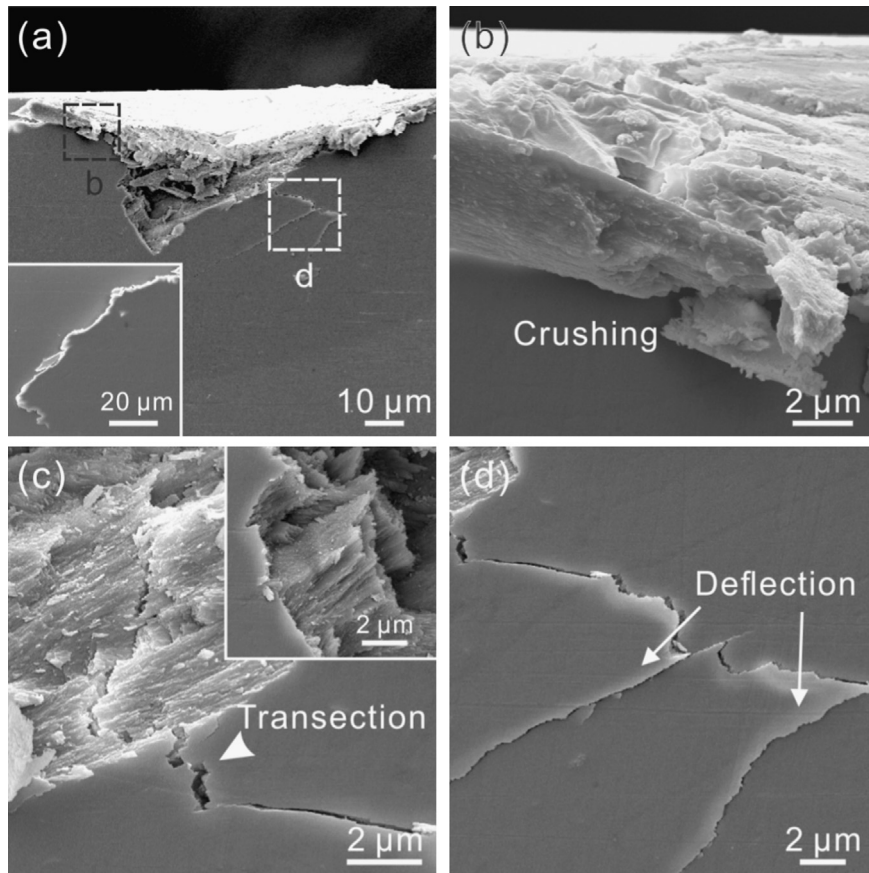


Fig. 9 – SEM micrographs of the outer enamel (a, b) and the P- (c, d) and D-zones (e, f) in the inner enamel after indentation under 200 gf load along the transverse direction. (b), (d) and (f) are magnified views of the square regions in (a), (c) and (e), respectively.



**Fig. 10** – SEM micrographs of giant panda's tooth enamel beneath the indenter after indentation under 200 gf load along the transverse direction. The inset in (a) shows the corner crack emanated from the left side of the crater. (b–d) show magnified views of representative morphologies manifesting the damage behavior.

2010b; He and Swain, 2008). With respect to positional dependence, the variations in hardness and indentation toughness along the enamel thickness result from chemical and structural gradients across the enamel. It has been revealed that the content of HAP minerals and their crystallinity decrease continuously from the occlusal surface to DEJ; while the organic content changes in the opposite manner in human tooth enamel (Cuy et al., 2002; Gutiérrez-Salazar and Reyes-Gasga, 2003; Xu et al., 2012). Similar compositional variations exist in the giant panda's tooth enamel (Fig. 8b). Additionally, along the transverse direction, the orientation of sheaths deviates gradually from being orthogonal to the loading direction with the increase of enamel thickness. Such varying structural orientations lead to continuous deflection and twisting of cracks, which represent a potent toughening and crack-arresting capability, giving rise to improved toughness of enamel.

The indentation damage behavior along different directions can be schematically illustrated in Fig. 11. The distinct features and their orientation dependence arise essentially from the notion that cracks in enamel invariably tend to propagate along interfaces rather than traversing them. On one hand, the enamel sheaths, which are less resistant to fracture than the rods (Ge et al., 2005), act as preferred channels for indentation damage, leading to the predominance of inter-rod cracks. Moreover, the unique arrangement

of rods in the decussation bands of inner enamel leads to continuous crack deflection and twisting along the interfaces, which confers significant resistance to the inward propagation of indentation damage. Additionally, at lower length-scales, the boundaries between HAP fibers and fiber bundles also provide preferred propagation paths for the intra-rod cracks that tend to be deflected along these boundaries.

#### 4.2. Toughening mechanisms

The enamel in the giant panda's tooth derives resistance to damage from a series of toughening strategies induced by its biologically hierarchical and graded structure. The organic matter, though accounts for a minimal fraction, is concentrated at the interfaces in the tooth enamel, leading to the preferential slippery and cracking along these interfaces (Bechtel et al., 2010a, 2010b; Xie et al., 2008; Yahyazadehfar and Arola, 2015). This helps activate a suite of extrinsic toughening mechanisms to resist the development of cracks and damage. Considering the indentation in the longitudinal direction, the deflection of radial-median cracks along the sheaths helps diminish the local stress intensity experienced at the crack tip. For an ideal crack subjected to tensile loading, the ratio of the effective (local) stress intensity  $K_{eff}$  for a simply (in-plane) deflected crack and the applied (global) stress intensity  $K_I$  is related by  $K_{eff}/K_I = \cos^2 \frac{\theta}{2}$  where  $\theta$  is the

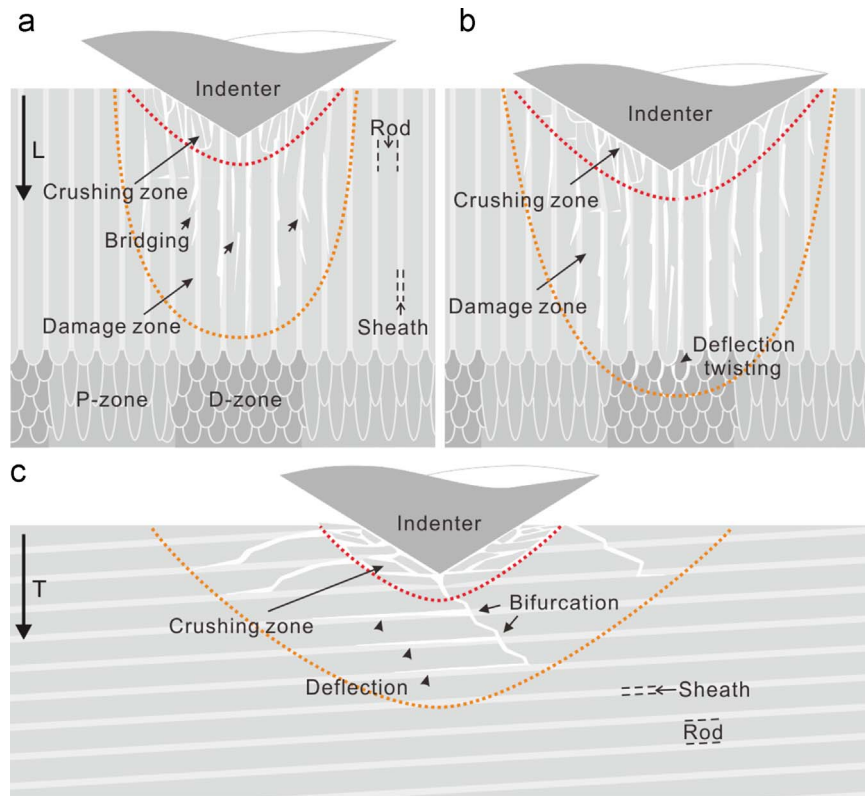


**Fig. 11 – Schematic illustrations of the damage behavior and toughening mechanisms of giant panda's tooth enamel under indentation along the longitudinal (a, b) and transverse (c) directions. For the longitudinal direction, the indentation damage is confined within the outer enamel in (a) and to extend into the inner enamel in (b) as the indentation load increases.**

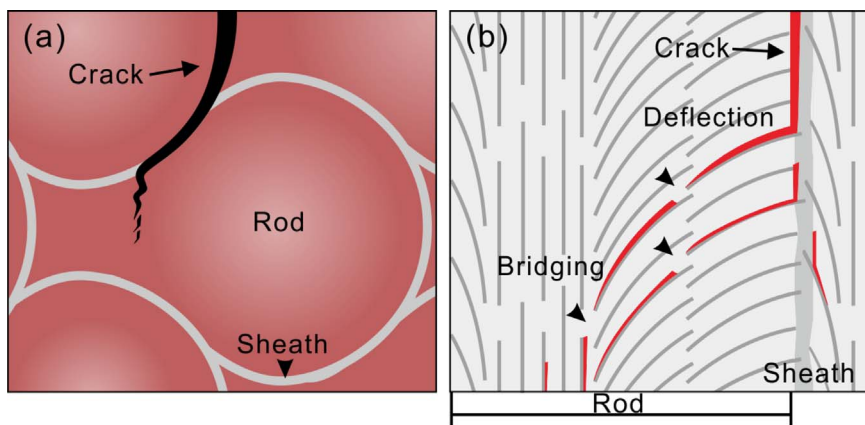


**Fig. 12 – Schematic illustrations of the penetration of an inter-rod crack into the rod at the necked rod tail (a) and the trapping of a crack into enamel rods along the boundaries between HAP fibers and the extrinsic toughening mechanisms that result (b).**

crack-deflection angle (Faber and Evans, 1983). Additionally, numerous bridges in form of intact rods or HAP fibers/fiber bundles act to span the cracks and further reduce the local stress intensity at the crack tip.

Specifically, the propagation of cracks within enamel rods is resisted by toughening mechanisms that are effective at the nano- to micro-scale, e.g., crack deflection along HAP fiber boundaries and bridging by uncracked fibers or fiber bundles. The cracks propagating along the sheaths may also be trapped by rods themselves from the following factors. Firstly, the keyhole-shaped cross-section of the enamel rods

leads to considerable resistance for the interfacial propagation of cracks. Accordingly, cracks may alternatively penetrate into the rods, especially in regions as the necked rod tails (Ang et al., 2011), as illustrated in Fig. 12a, and then be subjected to continuous deflection and consequent nanoscale bridging within the rods. Secondly, the sheaths are fairly uneven at the nanoscale and the HAP fibers extending from adjacent rods may be intercrossed there. As these fibers are tilted gradually from the sheaths towards the center of rods, cracks can be channeled along the fiber boundaries into the rods as avoiding or detouring around the fibers becomes

**Table 2 – Mechanical properties of giant panda's tooth enamel compared to those of human enamel and bamboo stems (Bajaj et al., 2010; Craig and Peyton, 1958; Gutiérrez-Salazar and Reyes-Gasga, 2003; Habelitz et al., 2001; Hassan et al., 1981; He et al., 2006; Imbeni et al., 2005; King, 2014; Mann and Dickinson, 2006; Park et al., 2008; Staines et al., 1981; Xu et al., 1998). The Young's moduli of *Pseudosasa japonica*, *Phyllostachys nigra*, and *Phyllostachys bissetii* bamboos were measured by 4-point bending (King, 2014). The fracture toughness  $K_{IC}$  of the bamboos was calculated from the work of fracture  $\gamma_f$  determined by scissors testing following the relation  $K_{IC} = \sqrt{2\gamma_f E}$  (Darvell et al., 1996; Jeronimidis, 1980; King, 2014; Tarou et al., 2005). The fracture toughness of tooth enamels was determined by indentation testing.**

Materials	Hardness	Young's modulus	Fracture toughness
<i>Pseudosasa japonica</i>	11.0 ± 2.4 MPa	1.3 ± 0.7 GPa	3.82 MPa m <sup>1/2</sup>
<i>Phyllostachys nigra</i>	8.6 ± 3.1 MPa	1.2 ± 0.2 GPa	5.01 MPa m <sup>1/2</sup>
<i>Phyllostachys bissetii</i>	13.9 ± 4.5 MPa	1.5 ± 0.6 GPa	4.17 MPa m <sup>1/2</sup>
Human tooth enamel	3.2–4.16 GPa	70–120 GPa	0.4–1.0 MPa m <sup>1/2</sup>
Giant panda's tooth enamel	3.37 ± 0.06 GPa	106 ± 4 GPa (L) 96 ± 1 GPa (T)	0.52–0.93 MPa.m <sup>1/2</sup>

more difficult, as illustrated schematically in Fig. 12b. As such, enhanced shielding effect is generated to arrest the inward development of indentation damage.

#### 4.3. Comparison to human tooth enamel and bamboo

Table 2 summarizes the mechanical properties of giant panda's tooth enamel and human tooth enamel as well as the stems of three kinds of bamboos that giant pandas feed on (Bajaj et al., 2010; Craig and Peyton, 1958; Darvell et al., 1996; Gutiérrez-Salazar and Reyes-Gasga, 2003; Habelitz et al., 2001; Hassan et al., 1981; He et al., 2006; Imbeni et al., 2005; Jeronimidis, 1980; King, 2014; Mann and Dickinson, 2006; Park et al., 2008a, 2008b; Staines et al., 1981; Tarou et al., 2005; Xu et al., 1998). Here the indentation on the occlusal surface was considered as it resembles the actual case of mastication. The toughness values of enamel and bamboo, though measured using different methods, are used for a first comparison. Despite the distinct living and food habits of humans and the giant panda, there appear to be no significant differences in the mechanical properties of their tooth enamels; they both possess similar chemical components with a similar structural arrangement. The difference in the mastication abilities between the two species is thus considered to lie in the macroscopic dimensions of their teeth and involved tissues, as well as the mechanical properties of other tissues, e.g., their dentin, alveolar bone and oral muscles.

The hardness and Young's modulus of the giant panda's tooth enamel are respectively ~300 and 80 times higher than bamboo stems; however, the fracture toughness of enamel is 4 to 10 times smaller, leading to a seeming contradiction as the tooth clearly “conquers” bamboos during mastication. This may be interpreted from the following aspects. Firstly, the enamel principally provides hardness, strength and wear resistance to the tooth. The fracture toughness of tooth originates primarily from the underlying dentin, of which the hardness and elastic modulus were measured to be 0.69 ± 0.07 GPa and 20.2 ± 1.8 GPa, respectively, using nanoindentation for the present giant panda's tooth, and the DEJ through which the enamel is ingeniously attached to the dentin (Bechtle et al., 2010a, 2010b). The dentin comprises much higher content of organic components than enamel and possesses remarkable fracture toughness and rising crack-growth-resistance behavior (Kruzic et al., 2003). The

different mechanical properties, e.g., hardness, Young's modulus, strength and toughness, of various tissues are combined in the entire tooth-periodontal ligament-alveolar bone complex via intelligent structural assemble, leading to synergetic effect for enhanced mastication function (Bechtle et al., 2010a, 2010b; Imbeni et al., 2005). Secondly, the bamboo foods of giant pandas are always much fresher and more hydrated than samples used for mechanical testing (King, 2014); as such, the mechanical properties are expected to be inferior with respect of their strong dependences on hydration for biopolymers (Jiang et al., 2012; Liu et al., 2015a, 2015b; Ramamurty et al., 2005). For example, an increase of moisture content by 1% can result in a decrease of 2.5 MPa in the compressive strength of Moso bamboo (Jiang et al., 2012). Additionally, the failure of bamboo during mastication is more likely dominated by the separation of bamboo fibers which occurs more easily compare to their fracture and sliding in mechanical testing (Low et al., 2006; Mitch et al., 2010). Thus, the measured fracture toughness of bamboo may overestimate its resistance to chewing.

## 5. Conclusions

By analyzing the structure and mechanical behavior of giant panda's tooth enamel, comparing this to those of human enamel and bamboo, their primary food, and exploring the salient toughening mechanisms involved, the following conclusions can be drawn:

- 1) The giant panda's tooth enamel possesses a hierarchical structure with enamel rods well aligned near the surface yet obliquely arranged to form alternated decussation bands in interior. Nano-sized hydroxyapatite (HAP) fibers are oriented along the long axis of rods in the center and tilted gradually towards the sheaths at the periphery within rods. The enamel exhibits a gradient in composition with decreasing mineral content from the occlusal surface to the dentin-enamel junction (DEJ).
- 2) The mechanical behavior of giant panda's tooth enamel under indentation depends on both the structural orientation and location within the enamel. The outer enamel possesses a higher hardness and indentation toughness along the transverse direction than in the longitudinal one.

The hardness decreases from the occlusal surface towards the DEJ, while the indentation toughness varies in the opposite manner.

- 3) Indentation cracks preferentially propagate along the interfaces, i.e., sheaths or boundaries of HAP fibers. Multiple extrinsic toughening mechanisms, e.g., crack deflection/twisting and uncracked-ligament bridging, act to shield the cracks from the applied stress. Intra-rod cracks are more easily arrested owing to the efficient extrinsic toughening at the nanoscale; the inter-rod cracks may be trapped into rods along the fibers, leading to improved damage resistance.
- 4) The structure and mechanical properties of the tooth enamels of humans and giant panda are similar despite their distinctly different living and food habits. Compared to bamboo, the panda's enamel is superior in hardness and Young's modulus, yet inferior in toughness. The mechanical superiority of giant panda's tooth against bamboo results from the unique combination of different tissues in the tooth-periodontal ligament-alveolar bone complex and the high degree hydration of the bamboo foods that the pandas eat.

## Acknowledgments

This work was supported by the National Natural Science Foundation of China, Grant nos. 51501190 and 51331007 (for ZYW, DJ and ZFZ), and by the Multi-University Research Initiative Grant no. AFOSR-FA9550-15-1-0009 from the Air Force Office of Scientific Research to the University of California Riverside, specifically through a subcontract to the University of California Berkeley (for ZQL and ROR).

## REFERENCES

- Amada, S., Untao, S., 2001. Fracture properties of bamboo. *Compos. B Eng.* 32, 451–459.
- Amada, S., Ichikawa, Y., Munekata, T., Nagase, Y., Shimizu, H., 1997. Fiber texture and mechanical graded structure of bamboo. *Compos. B Eng.* 28, 13–20.
- Amini, S., Miserez, A., 2013. Wear and abrasion resistance selection maps of biological materials. *Acta Biomater.* 9, 7895–7907.
- Ang, S.F., Schulz, A., Fernandes, R.P., Schneider, G.A., 2011. Sub-10-micrometer toughening and crack tip toughness of dental enamel. *J. Mech. Behav. Biomed. Mater.* 4, 423–432.
- Anstis, G., Chantikul, P., Lawn, B., Marshall, D., 1981. A critical evaluation of indentation techniques for measuring fracture toughness: I, Direct crack measurements. *J. Am. Ceram. Soc.* 64, 533–538.
- Bajaj, D., Arola, D., 2009. On the R-curve behavior of human tooth enamel. *Biomaterials* 30, 4037–4046.
- Bajaj, D., Nazari, A., Eidelman, N., Arola, D., 2008. A comparison of fatigue crack growth in human enamel and hydroxyapatite. *Biomaterials* 29, 4847–4854.
- Bajaj, D., Park, S., Quinn, G.D., Arola, D., 2010. Fracture processes and mechanisms of crack growth resistance in human enamel. *JOM* 62, 76–82.
- Barani, A., Keown, A.J., Bush, M.B., Lee, J.J.-W., Chai, H., Lawn, B.R., 2011. Mechanics of longitudinal cracks in tooth enamel. *Acta Biomater.* 7, 2285–2292.
- Bechtle, S., Fett, T., Rizzi, G., Habelitz, S., Klocke, A., Schneider, G. A., 2010a. Crack arrest within teeth at the dentinoenamel junction caused by elastic modulus mismatch. *Biomaterials* 31, 4238–4247.
- Bechtle, S., Habelitz, S., Klocke, A., Fett, T., Schneider, G.A., 2010b. The fracture behaviour of dental enamel. *Biomaterials* 31, 375–384.
- Braly, A., Darnell, L.A., Mann, A.B., Teaford, M.F., Weihs, T.P., 2007. The effect of prism orientation on the indentation testing of human molar enamel. *Arch. Oral Biol.* 52, 856–860.
- Cai, H., Kalceff, S., Lawn, B.R., 1994. Deformation and fracture of mica-containing glass–ceramics in Hertzian contacts. *J. Mater. Res.* 9, 762–770.
- Chai, H., Lee, J.J.-W., Lawn, B.R., 2011. On the chipping and splitting of teeth. *J. Mech. Behav. Biomed. Mater.* 4, 315–321.
- Chen, P., McKittrick, J., Meyers, M.A., 2008b. Biological materials: functional adaptations and bioinspired designs. *Prog. Mater. Sci.* 53, 1–206.
- Chen, P., Lin, A.Y.M., Lin, Y., Seki, Y., Stokes, A.G., Peyras, J., Olevsky, E.A., Meyers, M.A., McKittrick, J., 2008a. Structure and mechanical properties of selected biological materials. *J. Mech. Behav. Biomed. Mater.* 1, 208–226.
- Craig, R.G., Peyton, F.A., 1958. The microhardness of enamel and dentin. *J. Dent. Res.* 37, 661–668.
- Cui, F.Z., Ge, J., 2007. New observation of the hierarchical structure of human enamel, from nanoscale to microscale. *J. Tissue Eng. Regen. Med.* 1, 185–191.
- Cuy, J.L., Mann, A.B., Livi, K.J., Teaford, M.F., Weihs, T.P., 2002. Nanoindentation mapping of the mechanical properties of human molar tooth enamel. *Arch. Oral Biol.* 47, 281–291.
- Daculsi, G., Kerebel, B., 1978. High-resolution electron microscope study of human enamel crystallites: size, shape, and growth. *J. Ultrastruct. Res.* 65, 163–172.
- Darvell, B.W., Lee, P.K.D., Yuen, T.D.B., Lucas, P.W., 1996. A portable fracture toughness tester for biological materials. *Meas. Sci. Technol.* 7, 954–962.
- Faber, K.T., Evans, A.G., 1983. Crack deflection processes – I, theory. *Acta Metall.* 31, 565–576.
- Ge, J., Cui, F., Wang, X., Feng, H., 2005. Property variations in the prism and the organic sheath within enamel by nanoindentation. *Biomaterials* 26, 3333–3339.
- Gutiérrez-Salazar, M.P., Reyes-Gasga, J., 2003. Microhardness and chemical composition of human tooth. *Mater. Res.* 6, 367–373.
- Habelitz, S., Marshall, S.J., Marshall, G.W., Balooch, M., 2001. Mechanical properties of human dental enamel on the nanometer scale. *Arch. Oral Biol.* 46, 173–183.
- Haines, D.J., 1968. Physical properties of human tooth enamel and enamel sheath material under load. *J. Biomech.* 1, 117–125.
- Hassan, R., Caputo, A.A., Bunshah, R.F., 1981. Fracture toughness of human enamel. *J. Dent. Res.* 60, 820–827.
- He, L.H., Swain, M.V., 2008. Understanding the mechanical behaviour of human enamel from its structural and compositional characteristics. *J. Mech. Behav. Biomed. Mater.* 1, 18–29.
- He, L.H., Fujisawa, N., Swain, M.V., 2006. Elastic modulus and stress-strain response of human enamel by nano-indentation. *Biomaterials* 27, 4388–4398.
- Huang, W.P., 1993. The skull, mandible and dentition of giant pandas (*Ailuropoda*): morphological characters and their evolutionary implications. *Vertebr. Palasiat.* 31, 191–207.
- Imbeni, V., Kruzic, J.J., Marshall, G.W., Marshall, S.J., Ritchie, R.O., 2005. The dentin-enamel junction and the fracture of human teeth. *Nat. Mater.* 4, 229–232.
- Jeronimidis, G., 1980. The fracture behaviour of wood and the relations between toughness and morphology. *Proc. R. Soc. Lond. Ser. B* 208, 447–460.
- Jiang, Z., Wang, H., Tian, G., Yu, Y., 2012. Sensitivity of several selected mechanical properties of Moso bamboo to moisture

- content change under the fibre saturation point. *BioResources* 7, 5048–5058.
- Jiao, D., Liu, Z.Q., Zhang, Z.J., Zhang, Z.F., 2015. Intrinsic hierarchical structural imperfections in a natural ceramic of bivalve shell with distinctly graded properties. *Sci. Rep.* 5, 12418.
- Jung, Y.G., Peterson, I.M., Pajares, A., Lawn, B.R., 1999. Contact damage resistance and strength degradation of glass-infiltrated alumina and spinel ceramics. *J. Dent. Res.* 78, 804–814.
- King, R.A., 2014. Using *Ailuropoda melanoleuca* as a model species for studying the ecomorphology of *Paranthropus* (Master thesis). Marshall University, Department of Biology, Huntington.
- Koenigswald, W.V., Clemens, W.A., 1992. Levels of complexity in the microstructure of mammalian enamel and their application in studies of systematics. *Scanning Microsc.* 6, 195–217.
- Kruzic, J.J., Nalla, R.K., Kinney, J.H., Ritchie, R.O., 2003. Crack blunting, crack bridging and resistance-curve fracture mechanics in dentin: effect of hydration. *Biomaterials* 24, 5209–5221.
- Kruzic, J.J., Kim, D.K., Koester, K.J., Ritchie, R.O., 2009. Indentation techniques for evaluating the fracture toughness of biomaterials and hard tissues. *J. Mech. Behav. Biomed. Mater.* 2, 384–395.
- Li, L., Ortiz, C., 2014. Pervasive nanoscale deformation twinning as a catalyst for efficient energy dissipation in a bioceramic armour. *Nat. Mater.* 13, 501–507.
- Liu, Z.Q., Jiao, D., Meyers, M.A., Zhang, Z.F., 2015a. Structure and mechanical properties of naturally occurring lightweight foam-filled cylinder – the peacock's tail covert shaft and its components. *Acta Biomater.* 17, 137–151.
- Liu, Z.Q., Jiao, D., Zhang, Z.F., 2015b. Remarkable shape memory effect of a natural biopolymer in aqueous environment. *Biomaterials* 65, 13–21.
- Liu, Z.Q., Jiao, D., Weng, Z.Y., Zhang, Z.F., 2016. Structure and mechanical behaviors of protective armored pangolin scales and effects of hydration and orientation. *J. Mech. Behav. Biomed. Mater.* 56, 165–174.
- Low, I.M., Che, Z.Y., Latella, B.A., Sim, K.S., 2006. Mechanical and fracture properties of bamboo. *Key Eng. Mater.* 312, 15–20.
- Maas, M.C., Dumont, E.R., 1999. Built to last: the structure, function, and evolution of primate dental enamel. *Evol. Anthropol.* 8, 133–152.
- Macho, G.A., Jiang, Y., Spears, I.R., 2003. Enamel microstructure – a truly three-dimensional structure. *J. Hum. Evol.* 45, 81–90.
- Mann, A., Dickinson, M., 2006. Nanomechanics, chemistry and structure at the enamel surface. In: Duckworth, R.M. (Ed.), *The Teeth and Their Environment*. Basel, Karger, pp. 105–131.
- Martin, T., 1993. Early rodent incisor enamel evolution: phylogenetic implications. *J. Mamm. Evol.* 1, 227–254.
- Mitch, D., Harries, K.A., Sharma, B., 2010. Characterization of splitting behavior of bamboo culms. *J. Mater. Civ. Eng.* 22, 1195–1199.
- Mortell, J.F., Peyton, F.A., 1956. Observations of Hunter-Schreger bands. *J. Dent. Res.* 35, 804–813.
- Nanci, A., 2008. In: *Ten Cate's Oral Histology: Development, Structure, and Function* 8th ed. Elsevier, Missouri.
- Park, S., Quinn, J.B., Romberg, E., Arola, D., 2008a. On the brittleness of enamel and selected dental materials. *Dent. Mater.* 24, 1477–1485.
- Park, S., Wang, D.H., Zhang, D.S., Romberg, E., Arola, D., 2008b. Mechanical properties of human enamel as a function of age and location in the tooth. *J. Mater. Sci. Mater. Med.* 19, 2317–2324.
- Ramamurty, U., Jana, S., Kawamura, Y., Chattopadhyay, K., 2005. Hardness and plastic deformation in a bulk metallic glass. *Acta Mater.* 53, 705–717.
- Shang, J.K., Ritchie, R.O., 1989. Crack bridging by uncracked ligaments during fatigue-crack growth in SiC-reinforced aluminum-alloy composites. *Metall. Trans. A* 20A, 897–908.
- Staines, M., Robinson, W.H., Hood, J.A.A., 1981. Spherical indentation of tooth enamel. *J. Mater. Sci.* 16, 2551–2556.
- Tarou, L.R., Williams, J., Powell, D.M., Tabet, R., Allen, M., 2005. Behavioral preferences for bamboo in a pair of captive giant pandas (*Ailuropoda melanoleuca*). *Zoo Biol.* 24, 177–183.
- Wang, C., Li, Y., Wang, X., Zhang, L., Fu, B., 2012. The enamel microstructures of bovine mandibular incisors. *Anat. Rec.* 295, 1698–1706.
- White, S.N., Luo, W., Paine, M.L., Fong, H., Sarikaya, M., Snead, M.L., 2001. Biological organization of hydroxyapatite crystallites into a fibrous continuum toughens and controls anisotropy in human enamel. *J. Dent. Res.* 80, 321–326.
- Xie, Z., Swain, M., Munroe, P., Hoffman, M., 2008. On the critical parameters that regulate the deformation behavior of tooth enamel. *Biomaterials* 29, 2697–2703.
- Xu, C., Reed, R., Gorski, J.P., Wang, Y., Walker, M.P., 2012. The distribution of carbonate in enamel and its correlation with structure and mechanical properties. *J. Mater. Sci.* 47, 8035–8043.
- Xu, H.H.K., Smith, D.T., Jahanmir, S., Romberg, E., Kelly, J.R., Thompson, V.P., Rekow, E.D., 1998. Indentation damage and mechanical properties of human enamel and dentin. *J. Dent. Res.* 77, 472–480.
- Yahyazadehfar, M., Arola, D., 2015. The role of organic proteins on the crack growth resistance of human enamel. *Acta Biomater.* 19, 33–45.